Journal of Spinal Disorders
Vol. 7, No. 2, pp 130–138

Axes of Motion of Thoracolumbar Burst Fractures

T. R. Oxland, M. M. Panjabi, and R. M. Lin

Biomechanics Laboratory, Department of Orthopaedics and Rehabilitation, Yale University School of Medicine, New Haven, Connecticut, U.S.A.

Summary: The neurological injury associated with thoracolumbar burst fractures may be due to the acute trauma event or due to chronic instability. For functional diagnosis and appropriate treatment, knowledge of the altered motion patterns of burst fractures may be helpful. Thirteen human cadaveric spine specimens were impacted at high speed in axial compression, resulting in 10 clinically relevant burst fractures. The specimens were subjected to a three-dimensional flexibility test (flexion, extension, bilateral lateral bending, and bilateral axial torque) before and after trauma. The vertebral motion across the burst fracture was described in terms of the helical axis of motion (HAM), a set of parameters that concisely and completely describes the three-dimensional motion. The vertebral rotations about the HAM increased significantly with burst fracture in all loading directions: flexion 8.1–17.7°, extension 7.2–12.5°, lateral bending 8.5–20.6° (to one side), and axial torque 3.6–12.6° (to one side). The HAM shifted significantly in a posterior direction with burst fracture in flexion (11-mm shift), extension (15-mm shift), and axial torque (11-mm shift). No other significant shifts in the HAM position were observed. The translation along the HAM and the orientation of the HAM did not change significantly with injury in any of the loading directions. The results provide clinically relevant information regarding the optimal treatment of thoracolumbar burst fractures. Specifically, fixation methods for burst fractures must be particularly stiff in lateral bending and axial rotation, the directions of greatest instability. **Key Words:** Axes of motion—Burst fracture—Thoracolumbar injury.

Burst fractures total ~15% of all thoracolumbar injuries (4). In contrast to wedge compression fractures, they have potentially serious neurological consequences, including paraplegia, bowel dysfunction, severe low back pain, and sciatica. The frequency of neurologic deficit in patients with burst fracture has been reported to be as high as 60% (25).

There are two possible causes of neurological injury and deficit in burst fractures: (a) acute trauma during the fracture event, and (b) chronic instability. The potential for neurologic injury due to chronic instability of the fracture was emphasized previously (3). Chronic instability includes altered rigid body vertebral motion and deformations of the fractured vertebra(e) under load. The possibility of late neurologic damage may be significantly reduced if the fracture is properly stabilized. To provide sufficient stabilization to burst fractures, an adequate understanding of the intervertebral kinematics after the fracture must be attained. For example, it is important to provide rigid fixation in the directions of greatest instability.

Burst fractures have been studied experimentally by several research groups (5,6,11,18,22,23,26). The mechanical properties of the fractures have been studied less frequently. In the study by Willen et al., it was

Address correspondence and reprint requests to Dr. T. R. Oxland at his present address: Spine-Tech Inc., 980 East Hennepin Avenue, Minneapolis, MN 55414, U.S.A.

Dr. Lin's present address is Department of Orthopaedics, Cheng Kung University, Tainan, Taiwan.

shown that thoracolumbar burst fractures are very unstable injuries in flexion and tension/compression in comparison to the intact spine. To our knowledge, the complete three-dimensional characteristics of the burst fractures have not been described.

The purpose of the present study was to document the complete three-dimensional motion of experimentally produced thoracolumbar burst fractures in terms of the helical axes of motion (HAM), and compare the results with the intact behavior.

MATERIALS AND METHODS

Experimental Protocol

The overall experimental protocol is outlined as follows. The specimens were dissected and appropriately prepared for the mechanical testing procedures. The mechanical properties of the intact specimen were determined in the three-dimensional flexibility test. The specimen was subjected to one or more impacts in an attempt to produce a burst fracture. The three-dimensional flexibility test was repeated on the injured specimen to objectively assess the severity of the fracture. The injured specimen was radiographed [i.e., computed tomography (CT) scan and radiograph] to observe the fracture patterns. The specifics of each procedure are detailed in the following sections.

Specimen Preparation

Thirteen human cadaveric specimens (11 T11–L1, 2 T12–L2) were obtained and frozen in double plastic bags at −20°C. Lateral and anterior–posterior radiographs were taken of each specimen to ensure that no significant abnormalities were present. The ages of eight specimens were known and ranged from 19 to 70 years with an average age of 53 years. Each specimen was dissected of all nonligamentous soft tissue such as the spinal musculature and adjoining fascia. Care was taken not to damage any of the spinal ligaments or intervertebral discs. The rib articulations at T11 and T12 were left intact. The top and bottom vertebrae were mounted in polyester resin casts (Plastic Padding, Gothenburg, Sweden).

Three-Dimensional Flexibility Test

In the flexibility test, well-defined loads are applied to the free end of the specimen and the resulting rigid body displacements of the vertebrae are measured. The procedure described here is a well-established protocol used often at the Yale Biomechanics laboratory (13,27).

Rigid Plexiglas plates, each containing at least three noncollinear steel balls (1.6-mm diameter), were attached to the top and bottom casts with wood screws. Each marker, being a rigid extension of the vertebra, allowed measurement of the rigid body motion of the top vertebra with respect to the bottom.

Pure moments were applied to the top vertebra to ensure that the applied loads remained constant along the length of the specimen. Six pure moments, flexion, extension, left/right axial torque, and right/left lateral bending were applied individually in four equal steps to a maximum of 7.5 Nm. This load magnitude was selected such that it would not damage the specimen, especially after the trauma, but would produce motions that were in the physiologic range. The moments were applied in three load–unload cycles to precondition the specimen because it is a critical aspect of obtaining repeatable results in testing biological specimens (7). At each load step in each load cycle, the specimen was allowed 30 s of creep to reduce the viscoelastic effects of the spine.

At each step on the third loading cycle, stereophotographs were taken of the specimen with markers. The marker positions were digitized and the three-dimensional motions of the top vertebra with respect to the bottom vertebra (i.e., two intervertebral levels) were calculated using software developed in our laboratory. Total specimen motion was used rather than intervertebral motion because the injured vertebrae do not behave as rigid bodies. Therefore, using the motion of the top cast to bottom cast, i.e., two intervertebral levels, avoided this potential problem.

Parameters Studied

The three-dimensional rigid body motion of the top vertebra with respect to the bottom may be described in several ways. One common method involves three body rotations, typically Euler angles, and three translations of a single point on the vertebral body. This method suffers from the fact that Euler angles are sequence dependent and, therefore, there are six different possible values of each Euler angle for any rigid body motion (8). This problem is most evident in cases of large coupled vertebral motions. An alternative description of rigid body motion is the HAM. The HAM is a set of six parameters quantifying the three-dimensional motion. The HAM parameters are: orientation of the line (two parameters), a point of intersec-

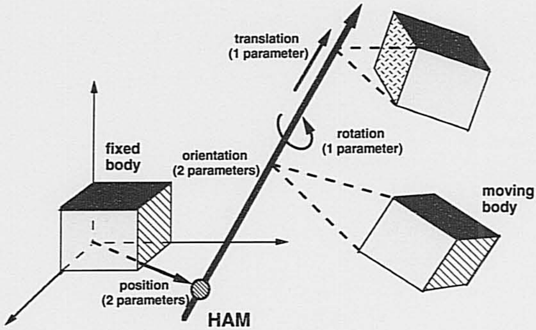

FIG. 1. Schematic representation of the helical axis of motion (HAM). Six unique parameters define the three-dimensional motion of a single rigid body: position of the HAM, orientation of the HAM, rotation of the HAM, and translation along the HAM.

tion with a particular plane (two parameters), a rotation of the rigid body about the axis (one parameter) and a translation of the rigid body along the axis (one parameter) (Fig. 1). For two-dimensional motions, the HAM is oriented perpendicular to the plane of motion and is analogous to the axis of rotation. For a more in-depth treatment of these alternative descriptions of rigid body motion, the reader should reference earlier works (8,10,16).

The magnitude of vertebral body motion was described in terms of HAM parameters of vertebral rotation and translation. The position of the HAM was described by its point of intersection with the coordinate system of the top vertebra. This coordinate system was established when the top vertebra was in the neutral position and it remained fixed in space. The orientation of the HAM was described by two angles: (a) a counterclockwise rotation about the y axis, i.e., longitude measured from the positive z axis, and (b) a subsequent clockwise rotation about the x axis (i.e., latitude) upward (+ve) or downward (−ve) (Fig. 2).

It is well known that intervertebral motion is nonlinear. One may consider it to be biphasic. To describe the nonlinear mechanical behavior under constant applied load, several motion parameters have been defined (13,14), specifically the neutral zone (NZ), elastic zone (EZ), and range of motion (ROM). The NZ is the residual deformation from an initial neutral position to the position under zero load on the third load cycle. The neutral position was defined as the point midway between flexion and extension rotations under zero load on the third load cycle. The EZ is the displacement from the end of the NZ to the position under maximum load. The ROM is the displacement from the neutral position to the position under maximum load and, therefore, is the sum of the NZ and EZ. In the present study, the HAM is calculated from the neutral position to the position under maximum load (i.e., ROM).

Impact Apparatus

The apparatus to produce the burst fracture consisted of a mass dropped from a height, thereby transferring its energy to the spine specimen. On top of the specimen was an assembly designed to provide a consistent interface between the impacting mass and the specimen. For the first five specimens, the initial impact mass was 8.3 kg from a height of 1.6 m. The mass

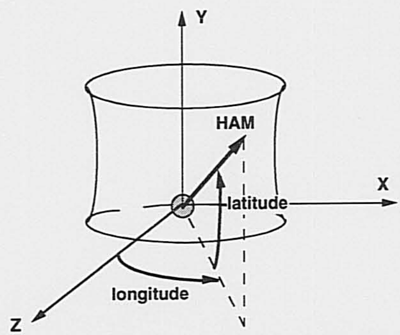

FIG. 2. The orientation of the helical axis of motion (HAM) was described in terms of two angles: (a) longitude, a counterclockwise (positive) rotation about the y axis, and (b) latitude, an upward (positive) rotation relative to the xz plane.

was increased in steps of 2 kg and the specimen was reimpacted, until the fracture occurred. A flat impact interface was used to prevent bending of the top vertebra in any vertical plane during the impact. The next two specimens used a cylindrical impact interface to allow sagittal rotation during impact. Because the compressive force was eccentric in this case, smaller impact masses were used. The initial impact mass was 2.3 kg from a height of 1.6 m, with an increment of 2 kg until the fracture. The final six specimens followed the same protocol as the first five specimens, except that the initial impact mass was 4.3 kg.

Statistical Analysis

The description of the HAM consists of six unique parameters, specifically the position of the axis (two coordinates), the orientation of the axis (two directions), and the vertebral rotation about and translation along the axis. Mean and standard error of the mean (SEM) were computed for each of these parameters. Comparisons between the intact and injured (i.e., burst fracture) states of the specimen were done using a paired Student's t test. For all tests, the null hypothesis was that there was no difference between the intact and injured groups. The results were evaluated at the 95% level of significance.

RESULTS

Of the 13 impacted specimens, 10 clinically relevant burst fractures were produced. There was no apparent relation between the burst fracture produced and the type of impact interface used. The burst fractures were verified by transaxial CT scans to have comminuted vertebral body with fracture of both the anterior and posterior walls of the vertebral body. A CT scan of a typical specimen is shown in Fig. 3.

All descriptions given below of the locations of the HAM are with respect to the specific coordinate system and its origin. The coordinate system is oriented with its x axis to the left, y axis upward, z axis anteriorly, and has its origin at the posterior, inferior corner of the upper vertebral body (Figs. 4–7). As mentioned earlier, the coordinate system was defined in the neutral position (i.e., midway between flexion and extension) of the specimen and it remained fixed in space.

Flexion

The changes in the HAM parameters in flexion are shown in Table 1. Vertebral rotation about the HAM increased significantly from intact to the burst fracture condition (8.1– 17.7°; $p < 0.0003$). The translations along the HAM in both the intact and burst fracture states were <1 mm and did not change significantly with injury (−0.8 mm intact, −0.1 mm injured).

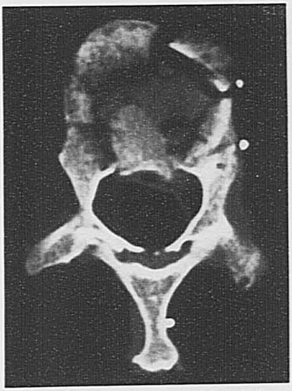

FIG. 3. Computed tomography scan of a typical experimental burst fracture.

The HAM was essentially perpendicular to the sagittal plane (i.e., longitude: 87.6° intact, 89.8° injured) because of the planar nature of the motion. The orien-

TABLE 1. *Helical axis of motion (HAM) parameters for the intact and burst fracture conditions in flexion and extension loading*

	Intact	Burst fracture	Significance
Flexion			
Rotation (deg.)	8.1 (0.8)	17.7 (1.5)	$p < .0003$
Translation (mm)	−0.8 (0.3)	−0.1 (0.3)	NS
Longitude (deg.)	87.6 (2.4)	89.8 (2.2)	NS
Latitude (deg.)	5.7 (3.9)	−1.6 (1.0)	NS
$y_{intercept}$ (mm)	−20.8 (3.1)	−26.1 (2.2)	NS
$z_{intercept}$ (mm)	13.3 (3.2)	2.1 (3.1)	$p < 0.03$
Extension			
Rotation (deg.)	7.2 (0.6)	12.5 (1.6)	$p < 0.03$
Translation (mm)	0.0 (0.1)	0.2 (0.2)	NS
Longitude (deg.)	89.5 (2.2)	91.6 (2.0)	NS
Latitude (deg.)	−2.4 (1.1)	−2.4 (1.1)	NS
$y_{intercept}$ (mm)	−27.1 (1.4)	−24.8 (1.8)	NS
$z_{intercept}$ (mm)	10.8 (2.1)	−4.3 (4.5)	$p < 0.007$

All values are mean (standard error of the mean). The y and z intercepts refer to the HAM intersections with the midsagittal plane. The statistical significance from paired Student's t tests are shown as NS for $p > 0.05$ and p values otherwise.

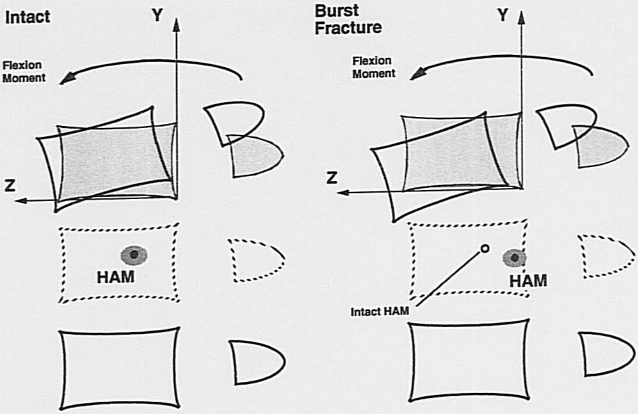

FIG. 4. Schematic diagram shows the sagittal plane position of the helical axis of motion (HAM) under an applied flexion moment for both the intact and burst fracture specimens. The shaded ellipses around the HAM are ±1 SEM.

tation of the HAM did not change significantly from the intact to the injured condition.

In the intact condition, the average position of the HAM in the midsagittal plane was 20.8 mm inferior (SEM 3.1 mm) and 13.3 mm anterior (SEM 3.2 mm) to the coordinate origin of the top vertebra (Fig. 4). Recall that the coordinate system origin is the posterior, inferior corner of the vertebral body. In the injured condition, the position of the HAM changed to 26.1 mm inferior (SEM 2.2 mm) and 2.1 mm anterior (SEM 3.1 mm) to the top vertebral origin. The change in the anterior–posterior position of the HAM was statistically significant ($p < 0.03$) whereas the superior–inferior shift was marginally significant ($p < 0.06$).

Extension

The changes in the HAM parameters in extension are shown in Table 1. The average vertebral rotation about the HAM increased significantly from intact (7.2°, SEM 0.6°) to the burst fracture condition (12.5°, SEM 1.6°) ($p < 0.03$). The translations along the HAM for the intact and injured were small (i.e., <0.5 mm) and did not change significantly with injury.

The HAM was essentially perpendicular to the sagittal plane (i.e., longitude: 89.5° intact, 91.6° injured) and this orientation did not change significantly with the burst fractures.

The average HAM for the intact specimen was located 27.1 mm inferior (SEM 1.4 mm) and 10.8 mm anterior (SEM 2.1 mm) to the origin of the coordinate system. In the injured condition, the position shifted to 24.8 mm inferior (SEM 1.8 mm) and 4.3 mm posterior (SEM 4.5 mm) to the top vertebra origin (Fig. 5). The anterior–posterior shift in the HAM position with injury was statistically significant (10.8 to −4.3 mm; $p < 0.007$). The slight increase in the superior–inferior position of the HAM was not statistically significant.

Axial Torque

The changes in the HAM parameters in left and right axial torque are shown in Table 2. The average axial rotation (i.e., average of left and right) about the HAM increased significantly from the intact to the burst fracture condition (3.6–12.6°; $p < 0.0001$). The translations along the HAM were small and did not change significantly with the burst fractures.

The average HAM was not perpendicular to any one of the three orthogonal anatomic planes. For the intact spine, the average longitude was 173.6° (SEM 18.8°) and latitude was 61.5° (SEM 3.0°). This is indicative of the coupled nature of the motion, specifically the simultaneous axial rotations and lateral bending due to the applied axial torque. With injury, the orientation of the HAM did not change significantly (i.e., injured longitude 159.7°, latitude 65.1°).

To describe the position of the HAM, its intersection with the transverse (horizontal) plane at the level

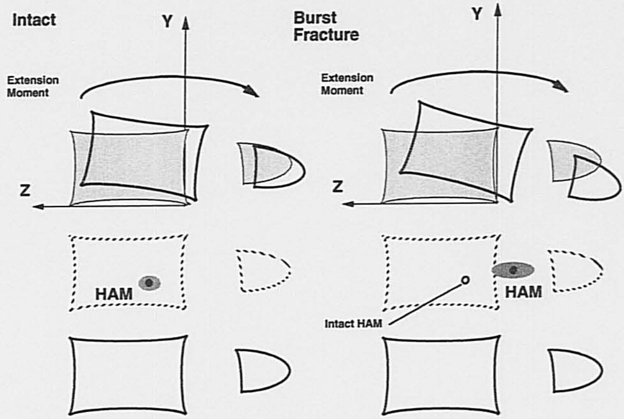

FIG. 5. Schematic diagram shows the sagittal plane position of the helical axis of motion (HAM) under an applied extension moment for both the intact and burst fracture specimens. The shaded ellipses around the HAM are ±1 SEM.

of the inferior endplate of the top vertebra was calculated. From the intact to the burst fracture condition, the position of the HAM moved posteriorly over 11 mm (0.66 to −10.6 mm), a statistically significant change ($p < 0.03$). A schematic representation of the HAM position in the transverse plane for left and right axial torque is shown in Fig. 6. There is an obvious posterior shift of the center of rotation from the

TABLE 2. *Helical axis of motion (HAM) parameters for the intact and burst fracture conditions in axial torque loading*

	Intact	Burst fracture	Significance
Left axial torque			
Rotation (deg.)	3.8 (0.5)	13.4 (3.2)	$p < 0.0001$
Translation (mm)	0.2 (0.2)	0.9 (0.3)	NS
Longitude (deg.)	123.5 (22.2)	122.1 (23.0)	NS
Latitude (deg.)	56.3 (5.0)	63.5 (3.7)	NS
$x_{intercept}$ (mm)	7.8 (8.1)	2.5 (4.4)	NS
$z_{intercept}$ (mm)	1.9 (7.0)	−9.6 (4.9)	NS
Right axial torque			
Rotation (deg.)	3.4 (0.3)	11.8 (2.2)	$p < 0.0001$
Translation (mm)	0.6 (0.2)	0.4 (0.5)	NS
Longitude (deg.)	223.7 (17.8)	197.3 (29.2)	NS
Latitude (deg.)	66.7 (2.8)	66.7 (3.1)	NS
$x_{intercept}$ (mm)	6.1 (3.4)	9.4 (3.7)	NS
$z_{intercept}$ (mm)	−0.6 (5.0)	−11.7 (5.2)	$p < 0.03$

All values are mean (standard error of the mean). The x and z intercepts refer to the HAM intersections with the transverse plane at the coordinate system origin. The statistical significance from paired Student's t tests are shown as NS for $p > 0.05$ and p values otherwise.

posterior vertebral wall in the intact specimens to ~10 mm into the spinal canal for the injured specimens.

Lateral Bending

The changes in the HAM parameters in right and left lateral bending are shown in Table 3. The average lateral rotation about the HAM increased significantly from the intact to the burst fracture state (8.5–20.6°; $p < 0.0001$). Translations along the HAM were small and did not change significantly with injury.

The average HAM was nearly perpendicular to the frontal plane (longitude: −3.4° intact, 1.0° injured). The orientation did not change significantly from intact to the burst fracture condition.

In the intact specimens, the HAM intersected the frontal plane at the level of the posterior wall of the vertebral body, ~20 mm inferior to the top vertebral coordinate origin (Fig. 7). For both right and left lateral bending, the intersection of the HAM with the frontal plane did not change significantly from the intact to the injured state.

DISCUSSION

In this article, the altered kinematics of a clinically important spine fracture were presented. Obviously, the findings are relevant only insofar as we could produce relevant thoracolumbar burst fractures. Of the 13 specimens, 10 were documented to have sustained

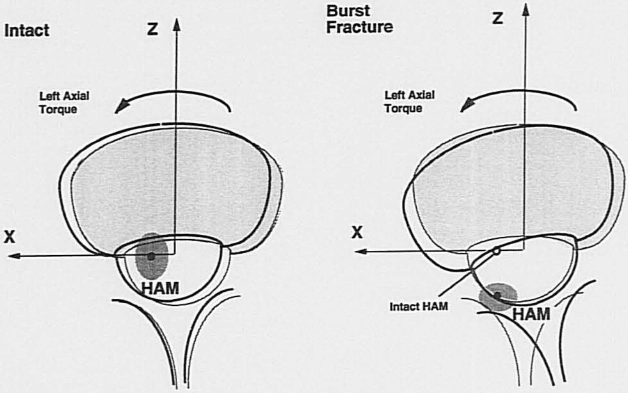

FIG. 6. Schematic diagram shows the transverse plane position of the helical axis of motion (HAM) under an applied left axial torque for both the intact and burst fracture specimens. The shaded ellipses around the HAM are ±1 SEM.

clinically relevant burst fractures. This judgment was based on Denis' definition of a burst fracture as that having disruption of both the anterior and posterior walls of the vertebral body. The results are limited to a certain extent by the fact that we have only 10 specimens, and therefore far-reaching conclusions cannot be made.

Experimental Methodology

Our approach was unique in both the dynamic nature of producing burst fracture and the use of the helical axis of motion (HAM) in describing the altered intervertebral mechanical behavior.

TABLE 3. *Helical axis of motion (HAM) parameters for the intact and burst fracture conditions in lateral bending loading*

	Intact	Burst fracture	Significance
Right lateral bending			
Rotation (deg.)	8.4 (0.7)	20.8 (2.4)	$p < 0.0001$
Translation (mm)	−0.3 (0.2)	−0.2 (0.3)	NS
Longitude (deg.)	4.6 (4.4)	5.0 (2.8)	NS
Latitude (deg.)	−1.1 (1.4)	−2.2 (1.2)	NS
$x_{intercept}$ (mm)	2.4 (1.9)	−2.6 (2.2)	NS
$y_{intercept}$ (mm)	−22.9 (1.4)	−24.0 (2.6)	NS
Left lateral bending			
Rotation (deg.)	8.6 (0.5)	20.5 (2.1)	$p < 0.0001$
Translation (mm)	−0.6 (0.2)	−0.7 (0.3)	NS
Longitude (deg.)	−11.3 (4.5)	−3.1 (3.0)	NS
Latitude (deg.)	−3.3 (1.1)	−3.9 (1.4)	NS
$x_{intercept}$ (mm)	8.9 (3.7)	7.1 (1.0)	NS
$y_{intercept}$ (mm)	−18.2 (2.5)	−23.3 (9.6)	NS

All values are mean (standard error of the mean). The x and y intercepts refer to the HAM intersections with the frontal plane at the coordinate system origin. The statistical significance from paired Student's t tests are shown as NS for $p > 0.05$ and p values otherwise.

The experimental production of burst fractures has been described previously. Some authors have adopted a high-speed impact approach on human specimens (26), whereas others have used less realistic methods including quasistatic loading (22) and stress-concentrating defects (23). We believe that the dynamic nature of the fracture mechanism without any artificial vertebral defects may be important in accurately quantifying the resultant instabilities.

In experimental studies of spinal injury, a significant problem is selecting an appropriate impact energy. The selection is made difficult by wide variation in the physical properties of the spine specimens. In the present experiment, the choice of an adequate drop mass and height was based on several factors. Both the mass and the height affect the magnitude of the impact energy. Only the drop height affects the velocity of the falling mass and, therefore, the rate at which the impact occurs. In previous studies of experimental spinal trauma, the rise times to peak force have ranged from 5 to 50 ms (9,21). In the present study, our goal was to achieve a rise time of ~5 ms. Preliminary studies suggested that a drop height of 1.6 m produced such a rise time. Our selection of the drop mass was guided by the previous studies that produced burst fractures. In those studies, initial potential energies ranged from 200 (26) to 300 J (5). To be on the conservative side of these energies, we selected a drop mass of 8.3 kg and drop height of 1.6 m, which corresponds to an impact energy of 130 J. This choice was based partially on our experience with producing

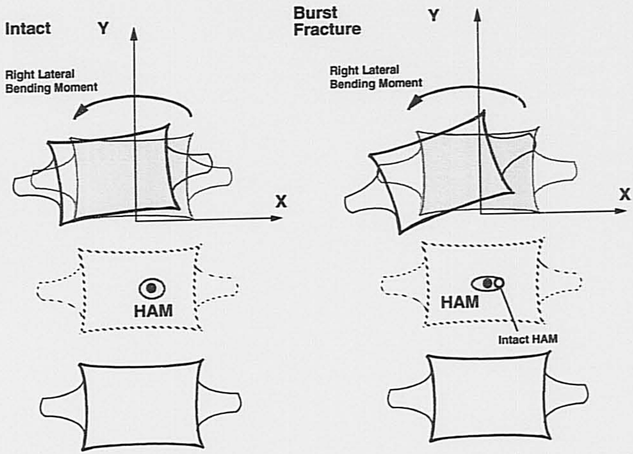

FIG. 7. Schematic diagram shows the frontal plane position of the helical axis of motion (HAM) under an applied right lateral bending moment for both the intact and burst fracture specimens. The shaded ellipses around the HAM are ±1 SEM.

spinal injury in human upper cervical (17) and porcine cervical spines (12,13,24).

To describe the three-dimensional motion of the burst fractures, we used the HAM concept. This method provides a complete description of the spinal motion. The magnitude of motion is quantified in terms of a single rotation about and a single translation along the HAM. The pattern of motion is described by the position of the HAM in any plane and the orientation of the HAM. The primary difficulty in the HAM concept is to communicate the six motion parameters in a simple manner. We have attempted to improve this by showing the HAM position in planes perpendicular to the applied moments, and using longitude and latitude to describe the HAM orientation.

Magnitude of Motion

The burst fractures exhibited significantly greater rotations than the intact spine in all directions of loading. The significant flexibilities in flexion and extension were consistent with the previous observations (11,23,26). The greatest increases were observed in lateral bending (250% of intact) and axial rotation (350% of intact). This was a similar finding to that observed previously (1).

These results are of significant interest to physicians in deciding on appropriate stabilization of burst fractures. The fixation method must be particularly effective in axial rotation and lateral bending. As an example, pedicle screw fixation is used frequently for burst fracture stabilization. Biomechanical testing of various pedicle screw systems has demonstrated that they are least stiff in axial rotation, when compared with the intact spine (20). Therefore, whenever pedicle screw fixation is used for burst fractures, those systems that provide the greatest stiffness in axial rotation are to be recommended.

Pattern of Motion

The position of the helical axis of motion for the vertebra adjacent to the burst fracture under applied moments shifted from the intact condition. In the intact state, the axis of rotation (HAM) in flexion and extension was in the posterior half of the middle vertebral body. This was slightly posterior to the findings in the thoracic spine (15) and similar to that observed in the lumbar spine (19). For the burst fractures, the HAM in flexion and extension shifted posteriorly such that it was almost coincident with the posterior vertebral wall in flexion (Fig. 4) and within the spinal canal in extension (Fig. 5). This posterior shift in the axis of rotation was indicative of the severe anatomic damage sustained anteriorly by the vertebra in burst fractures.

Under axial torque, the intact axis of rotation was essentially on the posterior vertebral wall, an observation that was consistent with previous findings (2) in

the lumbar spine. For both left and right axial torque, the HAM was to the left of the sagittal plane, indicating some asymmetry in the specimens. For the burst fractures, the axis of rotation shifted posteriorly into the posterior part of the spinal canal (Fig. 6). The severe vertebral body damage would explain this shift.

In lateral bending, the axis of rotation was in the midsagittal plane and within the middle vertebral body. With burst fracture, the HAM in lateral bending did not shift significantly.

The significant shifts in the HAM are indicative of altered kinematics of the spine due to the burst fracture. The posterior position of the HAM in flexion, extension, and axial rotation imply greater translations in the vertebral body, thereby increasing the potential for nonunions due to micromotions. Obviously, more rigid fixation will reduce the magnitude of such vertebral body translations and enhance the potential for proper bone healing.

Of particular interest was the proximity of the HAM to the spinal canal under flexion, extension, and axial torque for the burst fracture specimens. This position implies that translational movements in the spinal canal are reduced in specimens with burst fracture. Therefore, the late neurologic injury due to burst fracture instability is most likely not due to excessive rigid body motion around the neurologic structures. Rather, it is probably due to the deformations of fragments from the injured vertebra(e).

Acknowledgment: Support was provided in part by National Institutes of Health grant AR39209.

REFERENCES

1. Ching R, Tencer A, Anderson PA, Harrington RM, Daly CH: Residual in thoracolumbar spine fractures: A biomechanical study. Transactions of the Orthopaedic Research Society, San Francisco, 1993
2. Cossette JW, Farfan HF, Robertson GH, Wells RV: The instantaneous center of rotation of the third lumbar intervertebral joint. *J Biomech* 4:149–153, 1971
3. Denis F: The three column spine and its significance in the classification of acute thoracolumbar spinal injuries. *Spine* 8:817–831, 1983
4. Esses SI, Botsford DJ, Kostuik JP: Evaluation of surgical treatment for burst fractures. *Spine* 15:667–673, 1990
5. Fredrickson BE, Edwards WT, Rauschning W, Bayley JC, Yuan HA: Vertebral burst fractures: An experimental, morphologic and radiographic study. *Spine* 17:1012–1021, 1992
6. Fredrickson BE, Mann KA, Yuan HA, Lubicky JP: Reduction of the intracanal fragment in experimental burst fractures. *Spine* 13:267–271, 1988
7. Fung YC: *Biomechanics: Mechanical Properties of Living Tissue.* New York, Springer-Verlag, 1981
8. Goldstein H: *Classical Mechanics.* Reading, Massachusetts, Addison-Wesley, 1965
9. King AI, Prasad P, Ewing CL: Mechanism of spinal injury due to caudocephalad acceleration. *Orthop Clin North Am* 6:19–31, 1975
10. Kinzel GL, Hall AS, Hillberry BM. Measurement of the total motion between two body segments—I. Analytical development. *J Biomech* 5:93–105, 1972
11. Oxland TR: Burst fractures of the human thoracolumbar spine: A biomechanical investigation [Ph.D. Dissertation]. New Haven, Connecticut, Yale University, 1992
12. Oxland TR, Panjabi MM, Southern EP, Duranceau JS. An anatomic basis for cervical spine instability: A porcine trauma model. *J Orthop Res* 9:452–462, 1991
13. Panjabi MM, Duranceau JS, Oxland TR, Bowen CE: Multidirectional instabilities of traumatic cervical spine injuries in a porcine model. *Spine* 14:1111–1115, 1989
14. Panjabi MM, Goel VK, Summers D: Relationship between chronic instability and disc degeneration. ISSLS Proceedings, Toronto, Canada, 1982
15. Panjabi MM, Krag MH, Dimnet JC, Walter SD, Brand RA: Thoracic spine centers of rotation in the sagittal plane. *J Orthop Res* 1:387, 1984
16. Panjabi MM, Krag MH, Goel VK: A technique for measurement and description of three-dimensional six degree-of-freedom motion of a body joint with an application to the human spine. *J Biomech* 14:447–460, 1981
17. Panjabi MM, Oda T, Crisco JJ, Oxland TR, Katz L, Nolte L-P: Experimental study of atlas injuries. Part I: Biomechanical analysis of their mechanisms and fracture patterns. *Spine* 16:S460–S465, 1991
18. Panjabi MM, Oxland TR, Lin RM, McGowen TW: Thoracolumbar burst fracture: A biomechanical study of its multidirectional flexibility. *Spine* (in press)
19. Panjabi MM, Yamamoto I, Oxland TR, Crisco JJ: Helical axes of motion in the lumbar spine. Transactions of the Orthopaedic Research Society, Anaheim, California, 1991
20. Panjabi M, Yamamoto I, Oxland T, Crisco J, Freedman D: Biomechanical stability of five pedicle screw fixation systems. *Clin Biomech* 1991
21. Sances A Jr, Yoganandan N, Maiman DJ, et al.: Spinal injuries with vertical impact. In: *Mechanisms of Head and Spine Trauma,* ed by A Sances Jr, DJ Thomas, CL Ewing, SJ Larson, F Unterharnscheidt, New York, Aloray, 1986, pp 305–348
22. Shirado O, Kaneda K, Tadano S, Ishikawa H, McAfee P, Warden K: Influence of disc degeneration on mechanism of thoracolumbar burst fractures. *Spine* 17:286–292, 1992
23. Slosar P, Patwardhan A, Lorenz M, Havey R, Nixon R, Seymour S, Satori M: The three-dimensional instability patterns of the thoracolumbar burst fracture. ISSLS Proceedings, Chicago, Illinois, 1992
24. Southern EP, Oxland TR, Panjabi MM, Duranceau JS. Cervical spine injury patterns in three modes of high-speed trauma: A biomechanical porcine model. *J Spinal Disord* 3:316–328, 1990
25. Trafton PG, Boyd CA Jr.: Computed tomography of thoracic and lumbar spine injuries. *J Trauma* 24:506–515, 1984
26. Willen J, Lindahl S, Irstam L, Aldman B, Nordwall A: The thoracolumbar crush fracture. An experimental study on instant axial dynamic loading: The resulting fracture type and its stability. *Spine* 9:624–631, 1984
27. Yamamoto I, Panjabi MM, Crisco JJ, Oxland T. Three-dimensional movements of the whole lumbar spine and lumbosacral joint. *Spine* 14:1256–1260, 1989